ORNL/MD/LTR-185

MOX Average Power Intermediate PIE: 21 GWd/MT Quick Look

R.N. Morris
C.A. Baldwin
S.A. Hodge
C.M. Malone
N.H. Packan

March 2000

Fissile Materials Disposition Program

Notice

This report was prepared as an account of work sponsored by an agency of the United States Government. Neither the United States Government nor any agency thereof, or any of their employees, makes any warranty, expressed or implied, or assumes any legal liability or responsibility for any third party's use or the results of such use, of any information, apparatus, product or process disclosed in this report, or represents that its use by such third party would not infringe privately

Revision History

Revision number	Date Issued	Reason for revision
0	March 2000	First Issue

OAK RIDGE NATIONAL LABORATORY
MANAGED BY LOCKHEED MARTIN ENERGY RESEARCH CORPORATION
FOR THE U.S. DEPARTMENT OF ENERGY

BLDG. 3525, M/S 6295, ROOM 106
POST OFFICE BOX 2008
OAK RIDGE, TENNESSEE 37831-6295
TELEPHONE: 423-241-4237
FACSIMILE: 423-576-7862

March 2000

Distribution

MOX Average Power Intermediate: 21 GWd/MT Quick Look

The enclosed document details the MOX Average Power initial PIE that was performed on the intermediate-withdrawal Capsules 2 and 9 under the guidance of the DOE-sponsored Fissile Materials Disposition Program (FMDP). This work was carried out at the Irradiated Fuels Examination Laboratory by the staff of the Metals and Ceramics Division of the Oak Ridge National Laboratory during the period from October 1999 though March 2000. A final report of the entire PIE for these capsules is scheduled for issue in December 2000.

This is a Level-2 document as defined in the Fissile Materials Disposition Program Light-Water Reactor Mixed-Oxide Fuel Irradiation Test Project Plan, ORNL/MD/LTR-78

Sincerely,

Robert N. Morris
Fissile Materials Disposition Program

Enclosure

Distribution: See enclosure

ORNL/MD/LTR-185

MOX Average Power Intermediate PIE: 21 GWd/MT Quick Look

R.N. Morris
C.A. Baldwin
S.A. Hodge
C.M. Malone
N.H. Packan

March 2000

Oak Ridge National Laboratory

CONTENTS

LIST OF FIGURES iv

LIST OF TABLES vi

ACRONYMS vii

ABSTRACT viii

1. INTRODUCTION 1

2. SYNOPSIS OF IRRADIATION HISTORY AND CARTS PREDICTIONS 2
- 2.1 Irradiation History 2
- 2.2 Best Estimate CARTS Calculation Results 3
  - 2.2.1 In-Reactor Conditions at the End of the Phase II Irradiation 3
  - 2.2.2 Predicted Conditions in the Hot Cell 3
- 2.3 Summary and Conclusions from the CARTS Predictions 4

3. "QUICK LOOK" PRELIMINARY PIE 6
- 3.1 Capsule Photo Visual Inspection 6
- 3.2 Capsule Temperature Measurement 11
- 3.3 Capsule Dimensional Inspection 11
- 3.4 Capsule Gamma Scans 14
  - 3.4.1 Capsule 2 Gamma Scan 14
  - 3.4.2 Capsule 9 Gamma Scan 19
  - 3.4.3 Gamma Scanner Data Collection Orientation 24
- 3.5 Fission Gas Measurements 24
- 3.6 Fuel Pin Photo Visual Inspections 27
- 3.7 Fuel Pin Dimensional Inspections 31

4.0 CONCLUSIONS FROM PRELIMINARY PIE 33

5.0 ACKNOWLEDGMENTS 34

6.0 REFERENCES 35

7.0 DISTRIBUTION 36

FIGURES

Figure 1 Side view of Capsule 2 8

Figure 2 Top view of Capsule 2 8

Figure 3 Bottom view of Capsule 2 9

Figure 4 Top view of Capsule 9 9

Figure 5 Side view of Capsule 9 10

Figure 6 Bottom view of Capsule 9 10

Figure 7 Free air temperature measurement on Capsule 9 12

Figure 8 Schematic of diameter measurement 12

Figure 9 Capsule 2 mid energy gamma raster scan 15

Figure 10 Capsule 2 high energy gamma raster scan 16

Figure 11 Capsule 2 mid energy gamma line scan 17

Figure 12 Capsule 2 high energy gamma line scan 18

Figure 13 Capsule 9 mid energy gamma raster scan 20

Figure 14 Capsule 9 high energy gamma raster scan 21

Figure 15 Capsule 9 mid energy gamma line scan 22

Figure 16 Capsule 9 high energy gamma line scan 23

Figure 17 Orientation of the capsule and the gamma scanner collimator/detector 24

Figure 18 Cross sectional view of the Fission Gas Pressure Measuring Apparatus 25

Figure 19 Bottom end of Fuel Pin 5. Note the shortened pedestal from the cutting operation. 27

Figure 20 Top end of Fuel Pin 5. Note the hole from the fission gas pressure measurement 28

FIGURES (Cont)

Figure 21 Side view of Fuel Pin 5. Note capsule components in background 28

Figure 22 Bottom end of Fuel Pin 12. Note the shortened pedestal from the cutting operation 29

Figure 23 Top end of Fuel Pin 12. Note the hole from the fission gas pressure measurement. It also appears (top of hole) that the drill may have wandered or the pin may have rotated before the drill bit started cutting the hole. 30

Figure 24 Side view of Fuel Pin 12. Note capsule components in background 30

TABLES

TABLE 1 "Quick Look" Examination 6

TABLE 2 Capsule and Fuel Pin Numbers 7

TABLE 3 Capsule Temperature Measurements 11

TABLE 4 Capsule Measurements 13

TABLE 5 Fission Gas Measurements 26

TABLE 7 Fuel Pin Measurements 32

ACRONYMS

ATR	Advanced Test Reactor
FGPMA	Fission Gas Pressure Measuring Apparatus
FMDP	Fissile Materials Disposition Program
INEEL	Idaho National Engineering and Environmental Laboratory
LANL	Los Alamos National Laboratory
LHGR	Linear Heat Generation Rate
LWR	Light Water Reactor
MOX	Mixed Oxide
ORNL	Oak Ridge National Laboratory
PIE	Post Irradiation Examination
RG	Reactor Grade
TIGR	Thermally Induced Gallium Removal
WG	Weapons Grade

ABSTRACT

This report summarizes the early results of the post irradiation examination of the 21 GWd/MT MOX average power test capsules (numbers 2 and 9). The purpose of this preliminary examination is to document and monitor the progress of the MOX average power irradiation. The capsules and their fuel pins were found to be in excellent condition. Measurement of the fission gas release fraction (1.5 to 2.0%) and preliminary fuel stack gamma scan measurements indicate that the fuel is behaving as expected.

1. INTRODUCTION

This is the third report in a series of reports detailing the post irradiation examination (PIE) of the Fissile Materials Disposition Program (FMDP) Average Power MOX irradiation tests [Ref. 1]. These tests are investigating the use of weapons grade (WG) plutonium in mixed oxide (MOX) fuel for light-water reactors (LWR) to demonstrate that the substitution of weapons-derived plutonium for the reactor grade (RG) plutonium used in commercial MOX fuel does not negatively affect the performance of the fuel system and, thus, the commercial database is applicable. To meet this end, this test program was created to fabricate, assemble, and irradiate small test capsules containing weapons-derived MOX at expected fuel average power conditions, 6-10 kW/ft.

Simple, uninstrumented, drop-in capsules with local flux monitor wires were fabricated and placed in the Advanced Test Reactor (ATR) at Idaho National Environmental and Engineering Laboratory (INEEL). The average power test program comprises 13 capsules, 7 of which contain MOX fuel prepared without a gallium removal step, and 6 of which contain fuel prepared with a gallium removal step. The target irradiation goal is 30 GWd/MT for some capsules, but other capsules have been removed at 8 and 21 GWd/MT for the purpose of monitoring the irradiation, and two capsules have been designated as unirradiated archives. The topic of this report is the early examination of the two capsules that have been withdrawn after irradiation to 21 GWd/MT; two previous reports have dealt with the PIE at 8 GWd/MT [Refs. 2 and 3].

As before, the examination of the MOX capsules removed at 21 GWd/MT will be conducted in two steps. The first step is a “quick look” whose purpose is to determine the gross physical state of the capsule, cladding, and fuel. This first step is the topic of this report. The major goal of the quick look is to provide feedback to the irradiation group on issues that may impact the continued and safe operation of the capsules remaining in the ATR. This step also evaluates the usefulness of the current test apparatus and techniques for their role in the MOX irradiation task.

The second PIE step is a more detailed examination of the capsules for the purpose of collecting general cladding and fuel performance data for the FMDP program. The results of the second step PIE will be discussed in a final report for the intermediate-withdrawal PIE scheduled for issue in December 2000.

The general PIE plan is detailed in Ref. 4. However, modifications to this plan have taken place, especially in the areas of gallium analysis and clad testing, so the current FMDP PIE program manager should be consulted for details concerning the status of current PIE tasks.

2. SYNOPSIS OF IRRADIATION HISTORY AND CARTS PREDICTIONS

The intermediate-withdrawal PIE is performed on Capsules 2 and 9, which occupied the two lower front positions within the test assembly during Phases I and II of the average-power test irradiation. Predictions of fuel pin and pellet behavior are based upon results obtained with the Capsule Assembly Response – Thermal Swelling (CARTS) code. In essence, CARTS determines the quasi-steady state coupled thermal/mechanical solutions at each point in a series of stepwise advances in burnup. In addition to calculating the interplays between fuel swelling and fuel temperature, the CARTS models predict the temperature-induced radial dimension changes of the fuel pin and capsule, and the effects of fission gas release within the fuel pin. A more detailed description of CARTS operations is provided in Section 6.4 of Ref. 5.

2.1 Irradiation History

Phase I of the Average-Power Test extended from February 5 until September 13, 1998, and comprises ATR Cycles 115C through 117B. The CARTS code input for Capsules 2 and 9 during these periods of reactor operation represents the following linear heat generation rate (LHGR) history:

8.41 kW/ft from 0.00 to 2.78 GWd/MT Cycle 115C (48.4 EFPDs)
7.97 kW/ft from 2.78 to 3.45 GWd/MT Cycle 116A (12.8 EFPDs)
8.47 kW/ft from 3.45 to 4.70 GWd/MT Cycle 116B (22.2 EFPDs)
7.65 kW/ft from 4.70 to 5.42 GWd/MT Cycle 117A (14.1 EFPDs)
7.62 kW/ft f rom 5.42 to 8.34 GWd/MT Cycle 117B (57.4 EFPDs)

These LHGRs are averages of the as-run values for Capsules 2 and 9, which were in symmetric locations within the test assembly and remained in close agreement (difference < 0.6 percent).

There were two brief unplanned ATR shutdowns during Cycle 115C and one during Cycle 116A. Thus, the test capsules were thermally cycled eight times during the five ATR operation cycles of Phase I.

The Phase II irradiation began November 9, 1998, and continued until September 12, 1999, comprising ATR Cycles 118A through 120A. For these cycles, the CARTS code input for Capsules 2 and 9 represents the following LHGR history:

9.56 kW/ft from 8.34 to10.34 GWd/MT Cycle 118A(1) (27.5 EFPDs)
9.52 kW/ft from 10.34 to 11.44 GWd/MT Cycle 118A(2) (20.9 EFPDs)
9.41 kW/ft from 11.44 to 13.70 GWd/MT Cycle 118B (36.4 EFPDs)
7.05 kW/ft from 13.70 to 14.48 GWd/MT Cycle 119A(1) (19.0 EFPDs)
9.38 kW/ft from 14.48 to 14.67 GWd/MT Cycle 119A(2) (2.8 EFPDs)
9.24 kW/ft from 14.67 to 15.87 GWd/MT Cycle 119A(3) (22.8 EFPDs)
9.79 kW/ft from 15.87 to 18.15 GWd/MT Cycle 119B (42.1 EFPDs)
7.37 kW/ft from 18.15 to 20.93 GWd/MT Cycle 120A (56.2 EFPDs)

With two brief unplanned shutdowns during Cycle 118B and one during Cycle 120A, the test capsules were thermally cycled 11 times during the eight ATR operational cycles of Phase II.

These LHGR and accumulated burnups for Phases I and II are taken from the as-run MCNP code results obtained at INEEL after each ATR cycle. Uncertainties in these MCNP results are estimated to be +/- 2.5 percent. Combining the Phase-I and Phase-II experiences, Capsules 2 and 9 accumulated a total of 382.6 EFPDs with 19 thermal cycles. The burnup-averaged LHGR for these capsules is 8.56 kW/ft. The highest LHGR was 9.79 kW/ft near the end of Phase II.

2.2 Best Estimate CARTS Calculation Results

Since the internal dimensions and irradiation histories of Capsules 2 and 9 are virtually identical, the calculations were run (steps of 0.01 GWd/MT) for the Capsule 2 – Capsule 9 averages. The results are considered applicable to either capsule.

2.2.1 In-Reactor Conditions at the End of the Phase II Irradiation

It is of interest to consider the best-estimate results for pellet temperatures and diametral gaps during the last operating cycle just prior to removal of the intermediate-withdrawal capsules for PIE. While the calculated capsule wall temperature is almost independent of assumptions concerning the initial pellet-clad diametral gap and the extent of pellet densification, the calculated clad temperature is lower for pellets with minimum initial gaps. At the end of Phase II, the clad temperature (272-320°C) is much higher than the temperature (about 107°C) of the capsule wall, which is water-cooled on its outer surface. Further, the predicted mean pellet temperatures range from 508 to 621°C, so the pellets exhibit significant thermal expansion. (The pellet centerline temperatures range from 731 to 868°C.) Thus, although pellet-clad contact is not predicted to persist in the hot cell, periods of pellet-clad contact are expected to have occurred while the pellets were at elevated temperatures during reactor operation.

The best-estimate CARTS code predictions of pellet-to-clad diametral gaps just prior to reactor shutdown from Cycle 120A range from zero to 0.28 mils. The accompanying clad mechanical strains range from 0.05 percent to zero. (The largest mechanical strain at any time during the irradiation occurs for the case of zero pellet densification and minimum initial pellet-clad diametral gap, for which the maximum predicted mechanical strain is 0.15 percent.) When thermal strains are added, the total clad strain just before shutdown is predicted to lie in the range from 0.24 to 0.14 percent.

2.2.2 Predicted Conditions in the Hot Cell

After advancing the calculation through each of the ATR irradiation cycles, the final calculation step represents conditions in the hot cell. The MOCUP protocol (coordinating calculations by MCNP and ORIGEN) has been applied at INEEL to predict isotopic inventories and decay powers as documented in Ref. 6.

The CARTS predictions for the capsule conditions at the expected time of opening are based on a total decay power in the 15 pellets of 2.0 watts (0.0040 kW/ft), which corresponds to mid-January

2000. Heat transfer from the outer capsule surface is by free convection to the hot cell atmosphere. The natural convection heat transfer coefficient based on the capsule surface area directly over the six-inch pellet stack has been established as 27.1 W/m^2-°C (4.70 Btu/hr-ft^2-°F).

At the time the capsules are opened, the pellet-to-clad diametral gaps within the fuel pins are expected to lie in the range from 0.78 to 1.52 mils. Within this range, the gaps associated with the fifteen individual pellets vary according to the extent of pellet densification (zero to 0.50 percent) and the width of each pellet's initial cold diametral gap, which the design tolerances allow to lie between 2.0 and 3.5 mils.

The gas pressure within the fuel pins (based on the plenum volume associated with a nominal six-inch pellet stack length) is predicted to be 27.5 psia (12.9 psig). The corresponding assumed best-estimate release of gas (krypton and xenon) from the fuel matrix is 1.2 percent.

The diametral gap between the outer surface of the zircaloy clad and the inner surface of the stainless steel capsule is expected to lie between 2.1 and 3.1 mils. This one-mil range strictly follows from the design tolerances, which permit the cold clad-to-capsule initial diametral gap to vary between 2.0 and 3.0 mils. It is interesting to note that the predicted gaps are slightly larger than the gaps associated with the initial cold dimensions. This is because the clad and capsule wall are at very nearly the same temperature (about 43.3°C) in the hot cell, and the coefficient of expansion for steel is about three times larger than that of zircaloy. (The thermal strains for the capsule and fuel pin are 0.03 percent and 0.01 percent, respectively.)

2.3 Summary and Conclusions From The CARTS Predictions

The 15 pellets in each intermediate-withdrawal fuel pin are expected to exhibit, under hot cell conditions, diametral gaps ranging from 0.78 to 1.52 mils.

The diametral gap between the fuel pin and the capsule is expected to lie between 2.1 and 3.1 mils, which is slightly larger than the range for the initial cold capsule assemblies.

These results suggest that fuel pin removal from the capsule and the subsequent fuel pin disassembly should be straightforward, without significant interference from either pin-to-capsule or pellet-to-clad contact.

The gas pressure within the fuel pins is predicted to be about 27.5 psia (12.9 psig). However, this is based on a nominal pellet stack length and the calculated pressure would be proportionally less for a shorter pellet stack (and the associated longer gas plenum). Another consideration is that these pellets have experienced nineteen thermal cycles, which might induce increased gas release from the fuel matrix.

Although pellet-clad contact is not expected to be found when the fuel pins are opened in the hot cell, it is believed that pellet-clad contact did occur during Phase II of the irradiation. This is an important difference between the intermediate-withdrawal and early-withdrawal PIEs, since it is known that pellet-clad contact did not occur during Phase I.

The largest mechanical strain predicted to have occurred during irradiation is 0.15 percent, which is insufficient to cause yielding of the clad zircaloy. Thus, no residual mechanical strain is predicted for the clad in the hot cells.

3. "QUICK LOOK" PRELIMINARY PIE

Table 1 details the items that have been selected for Step I of the PIE effort. Note that these items form a subset of the total PIE effort. The capsules made available for the intermediate PIE effort are Capsule 2 (fuel prepared without gallium removal) and Capsule 9 (fuel prepared with gallium removal).

TABLE 1
"Quick Look" Examination

No.	Examination	Comments
1	Capsule photo visual	Containment integrity is major interest.
2	Capsule temperature measurement	Compare measured temperatures with predictions.
3	Capsule dimensional inspection	Containment integrity is major interest.
4	Capsule gamma scan	Determine gross internal state of capsule and fuel pin.
5	Fission gas sampling	The fission gas pressure and ^{85}Kr content of both the containment and the fuel pin will be analyzed.
Remove fuel pin from capsule		
6	Fuel pin photo visual	First assessment of clad integrity. (An additional gamma scan may be performed if the situation warrants.)
7	Fuel pin dimensional inspection	First assessment of clad integrity.

Note that the capsule and fuel pin numbering are not the same; Table 2 details the relationship between the two and identifies the status with respect to gallium removal treatment.

3.1 Capsule Photo Visual Inspection

The first portion of the PIE effort was to visually examine the capsule surfaces at low magnification. Both capsules appeared to be clean and bright with no sign of corrosion or damage. The black lines near the welding border are the heat-affected zone and are unrelated to the irradiation. In general, the stainless steel containment survived the irradiation as expected and these capsules appear no differently than the capsules removed at 8 GWd/MT. Photographs of these capsules are shown in Figures 1 through 6 for a variety of views. The two appear identical except for the identification marks.

TABLE 2
Capsule and Fuel Pin Numbers

Capsule Number	Fuel Pin Number	Fuel Batch	Gallium Treatment	Exposure (GWD/MT)	PIE Status
1	2	A	None	8	Largely complete - awaiting clad testing
2	5	A	None	21	Underway - subject of this report
3	6	A	None	In reactor	
4	7	A	None	In reactor	
5	8	A	None	In reactor	
6	9	A	None	In reactor	
7	10	A	None	Unirradiated archive	
8	11	B	Thermal (TIGR)	8	Largely complete - awaiting clad testing
9	12	B	Thermal (TIGR)	21	Underway - subject of this report
10	13	B	Thermal (TIGR)	In reactor	
11	14	B	Thermal (TIGR)	Unirradiated archive	
12	15	B	Thermal (TIGR)	In reactor	
13	16	B	Thermal (TIGR)	In reactor	

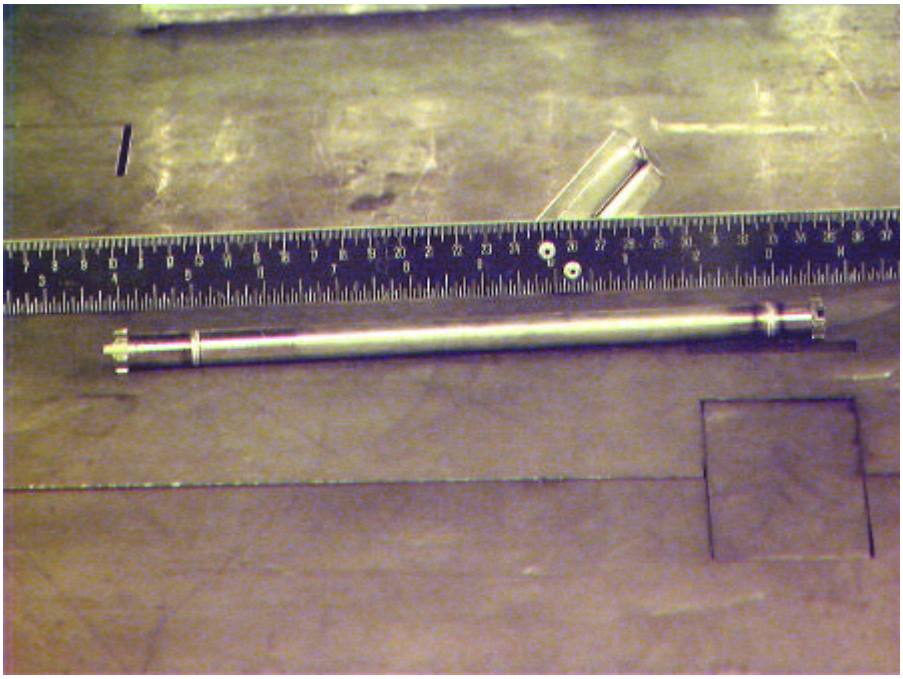

Figure 1 Side view of Capsule 2. [R2-side-front.JPG]

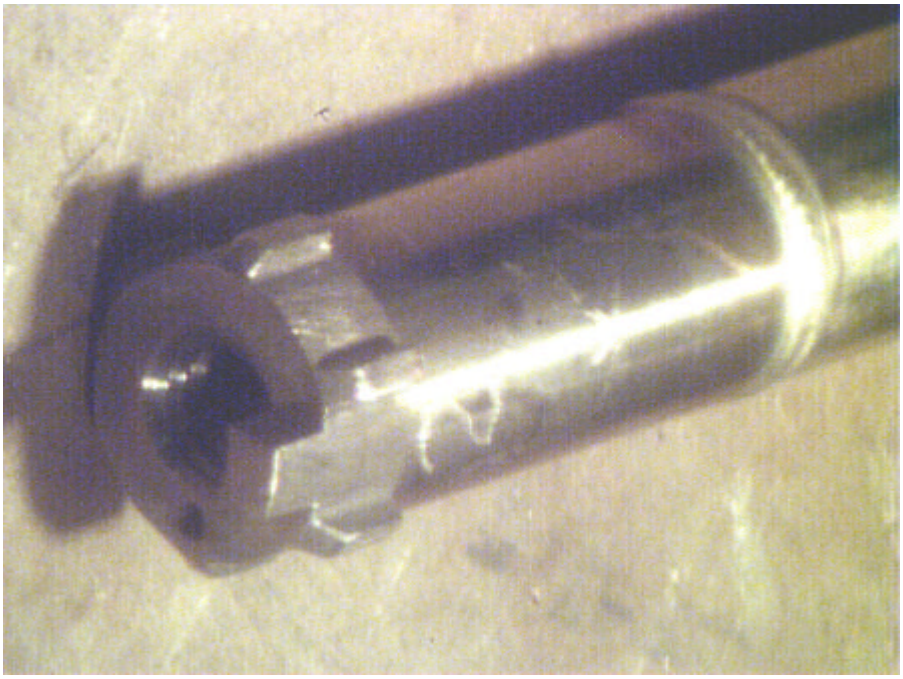

Figure 2 Top view of Capsule 2. [R2-top-high.JPG]

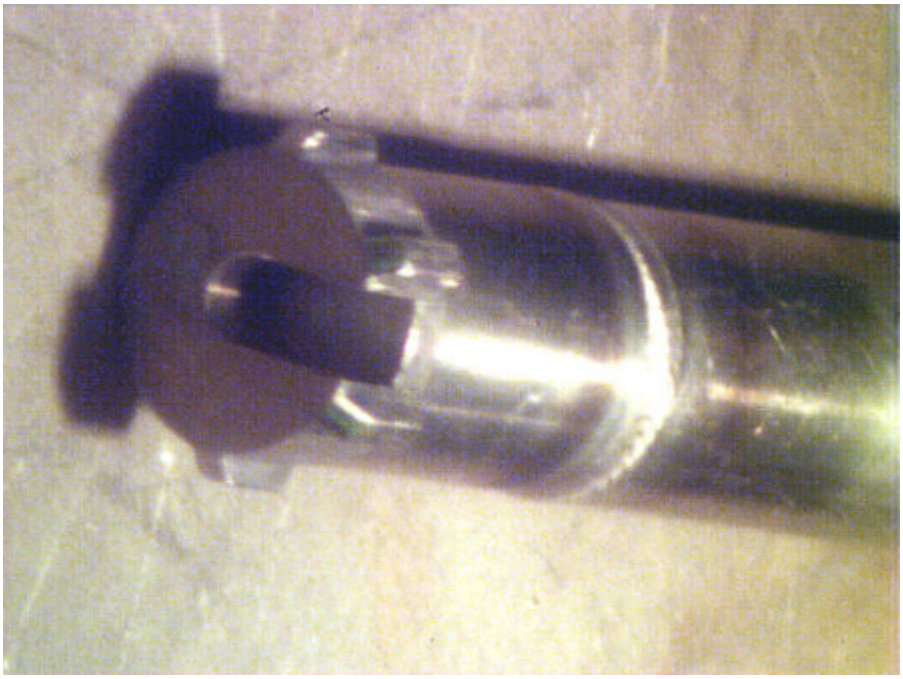

Figure 3 Bottom view of Capsule 2. [R2-bot-high.JPG]

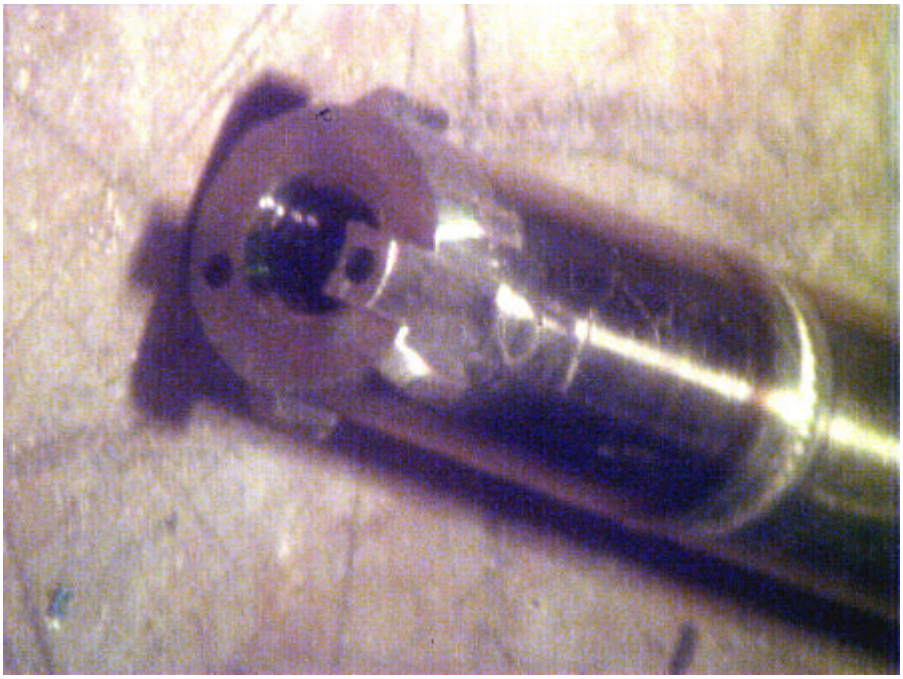

Figure 4 Top view of Capsule 9. [R9-top-high.JPG]

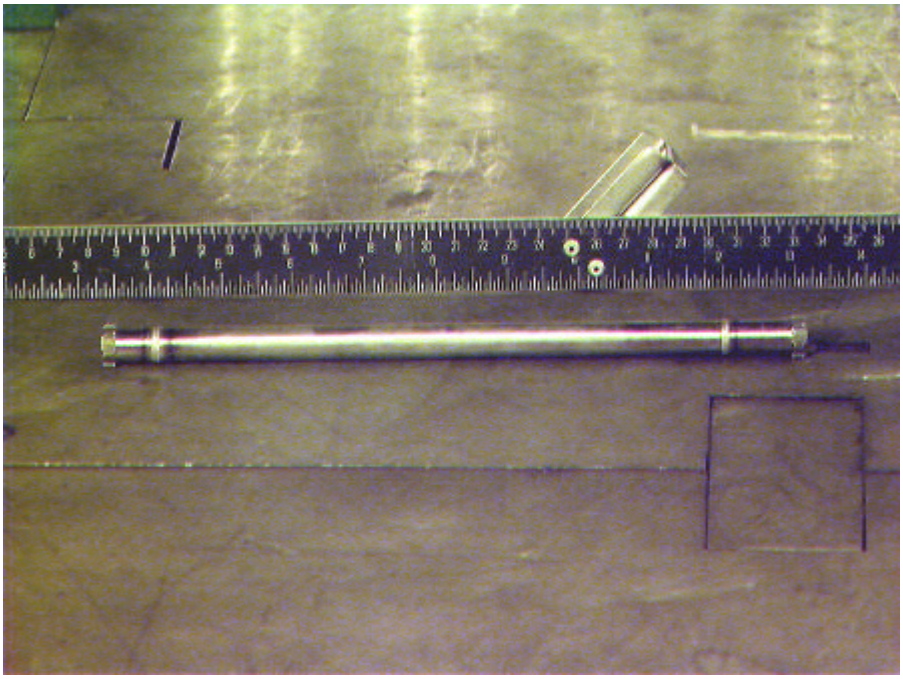

Figure 5 Side view of Capsule 9. [R9-side-front.JPG]

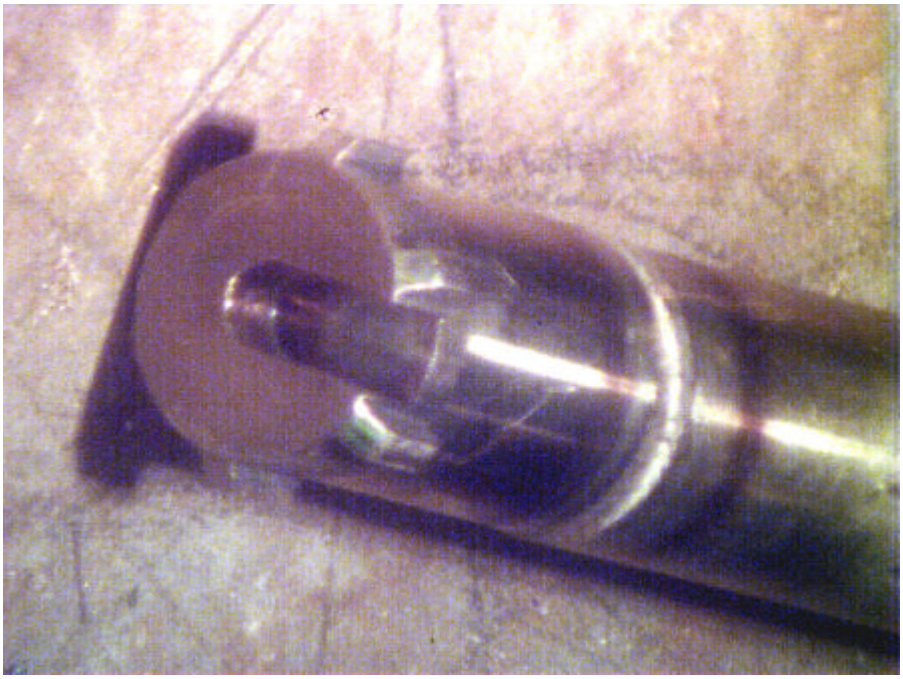

Figure 6 Bottom view of Capsule 9. [R9-bot-high.JPG]

3.2 Capsule Temperature Measurements

The temperature measurements and their locations as taken on Capsules 2 and 9 are shown in Table 3. A photo of a capsule undergoing a measurement is shown in Fig. 7. The apparatus consists of a Type C thermocouple held to the capsule by a modified hose clamp.

TABLE 3 **Caspule 2 and 9 Temperature Measurements**	
MOX Capsule 2	
Measurements taken on 10/27/99 from 0930 to 1345	
Top Weld	101.4°F (38.7°C)
Mid Point	125.4°F (51.8°C)
Bottom Weld	112.4°F (44.5°C)
Average	*113.1°F (45.0°C)* *43.3°C predicted in Section 2.2*
Cell Ambient	86.0°F (30°C)
MOX Capsule 9	
Measurements taken on 10/26/99 from 0910 to 1230	
Top Weld	102.4°F (39.0°C)
Mid Point	127.6°F (53.2°C)
Bottom Weld	108.6°F (42.5°C)
Average	*112.8°F (44.9°C)* *43.3°C predicted in Section 2.2*
Cell Ambient	86.4°F (30.2°C)

Notes :
Temperature measurements were taken 10" from the hot cell table top and allowed to stabilize for 45 minutes. Fahrenheit and Centigrade values were determined by switching between instrument readouts, not mathematical conversion.

3.3 Capsule Dimensional Inspection

The results of the stainless steel capsule dimensional inspections are shown in Table 4. Within 0.001 inches, there were no indications of bowing, out of roundness, or bambooing (distortions in the clad where the pellets meet). Measurements for bowing and bambooing were carried out between the capsule welds. Only a slight difference between pre and post irradiation diametrical values was noted, less that 0.001 inches, which could be due to radiation induced changes and/or thermal expansion due to the somewhat higher measurement temperature in the hot cell. The lengths of the

capsules were found to agree with the preirradiation values within 0.007 inches. Figure 8 details the measurement method for radial dimensions.

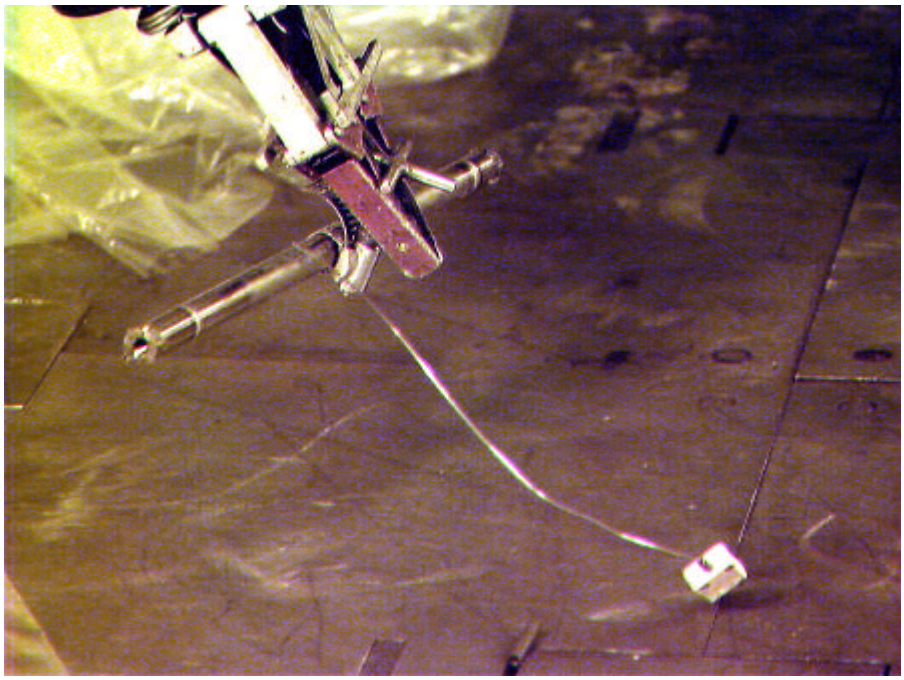

Figure 7 Free air temperature measurement on Capsule 9.
[R9-temprt.JPG]

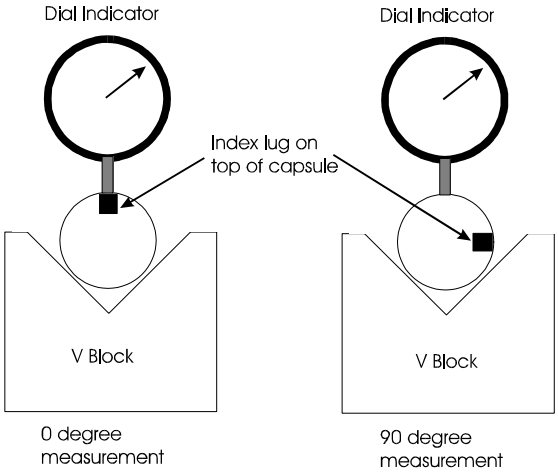

Figure 8 Schematic of diameter measurement.
[vblock.wpg]

TABLE 4 Capsule Measurements			
Axial Location	**Diameter Measurement (in) (±0.0005 in)**		**Preirradiation Value (in)**
	0°	**90°**	
Capsule 2			
3.9" from capsule top	0.4653	0.4651	0.4643 to 0.4649
Center of capsule	0.4656	0.4653	
6.7" from capsule top	0.4654	0.4652	
Capsule 9			
4.0" from capsule top	0.4651	0.4650	0.4643 to 0.4649
Center of capsule	0.4652	0.4648	
6.5" from capsule top	0.4653	0.4652	
Length (in) (±0.005 in)			
Capsule 2	9.585		9.578 after welding (9.59 before welding)
Capsule 9	9.581		9.576 after welding (9.59 before welding)
Mass (g) (±0.1 g)			
Capsule 2	192.3		Not given
Capsule 9	192.8		Not given

3.4 Capsule Gamma Scans

Both Capsules 2 and 9 were raster scanned to obtain a two dimensional view of the capsule internal structure. These scans were composed of just over 5000 points and were taken with a 1/16" diameter collimator in two energy ranges. The range 400 to 700 KeV was employed to broadly cover the fission products while the range 800 to 1575 keV was used to broadly cover the activation products. These two energy ranges were selected because they show the most details of interest for a general view.

An effort was made to detect the free ^{85}Kr inventory in the plenum region of the fuel pin contained in Capsule 9 using the gamma scanner, but no ^{85}Kr could be observed due to the high background from other isotopes.

In addition, both capsules underwent an axial line scan (400 points) along their length using the same collimator as was used in the two-dimensional scans. Results from these two energy ranges are presented in the following sections. Overall, the capsules appeared to be intact with no unusual structure or abnormalities.

It should be noted that the resolution of the gamma scanner has been improved (from that used for the 8 GWd/MT PIE) by increasing the length of the collimator and reducing the distance between the capsule and the collimator. These improvements have resulted in significantly better resolution as can be seen by the squareness of the edges on the pellets as seen in Figures 9 and 13.

3.4.1 Capsule 2 Gamma Scan

Figure 9 shows the result of the 400 to 700 KeV raster scan for Capsule 2. When compared to the schematic above it, one can make out the stainless steel end caps, the fuel pin end caps, and very clearly, the fuel pellet stack. The pedestal on the lower fuel pin plug is vaguely outlined as well as is the capsule boundary (the capsule bottom is to the left, the top to the right). Figure 10 shows the same scan in the 800 to 1575 keV energy range. This higher energy range outlines the stainless steel components to a greater degree.

The schematic in Figure 9 and in the following Figures is based on the nominal capsule design. This design has a fuel stack length of 6.0 inches. The drawings are scaled so that the stack height in both the schematic and the data match. In reality, the fuel stack length is slightly less than 6.0 inches (about 5.8 inches), so that a small misalignment between the components of the two is apparent to the careful reader in some cases. The fuel stack had a tolerance of +0.00, -0.20 inches, so this is normal. Actual dimensions are listed in Table 2.1 of Reference 3.

Figure 11 shows an axial line scan along the capsule in the 400 to 700 keV energy range. Again, the elements of the capsule are clearly indicated. The fuel pellet stack appears to be about 5.8 inches long. Note the burnup peaking at the ends of the fuel stack and the signal dips indicating the dished ends of the 15 pellets.

Figure 12 shows an axial line scan in the energy range of 800-1575 KeV, which accents the stainless steel activation products. This figure shows the stainless steel capsule end caps and wall more clearly. The fuel can be seen because of the high energy fission product emitters such as ^{140}La.

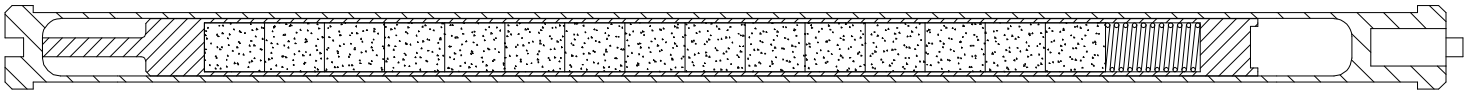

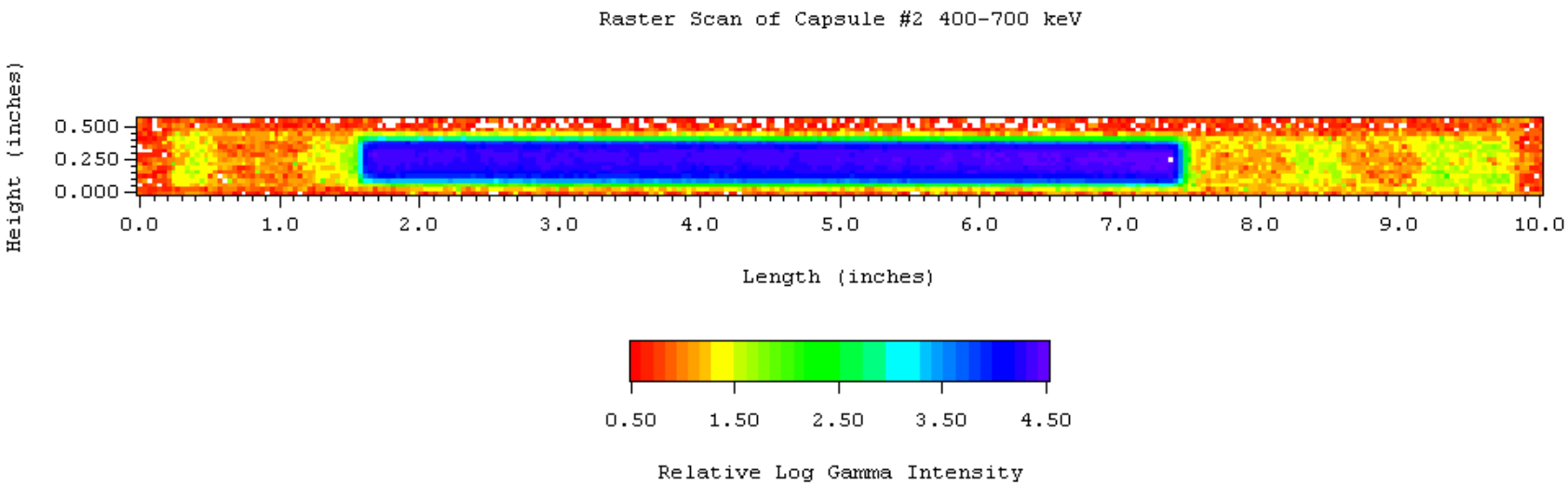

Figure 9 Capsule 2 mid energy gamma raster scan. [ras2.wpg]

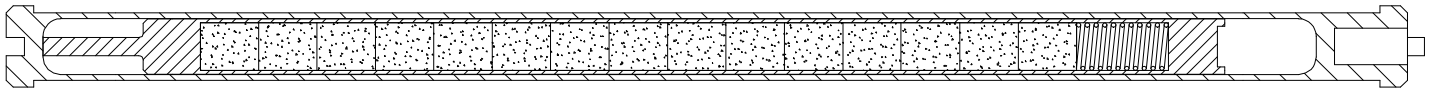

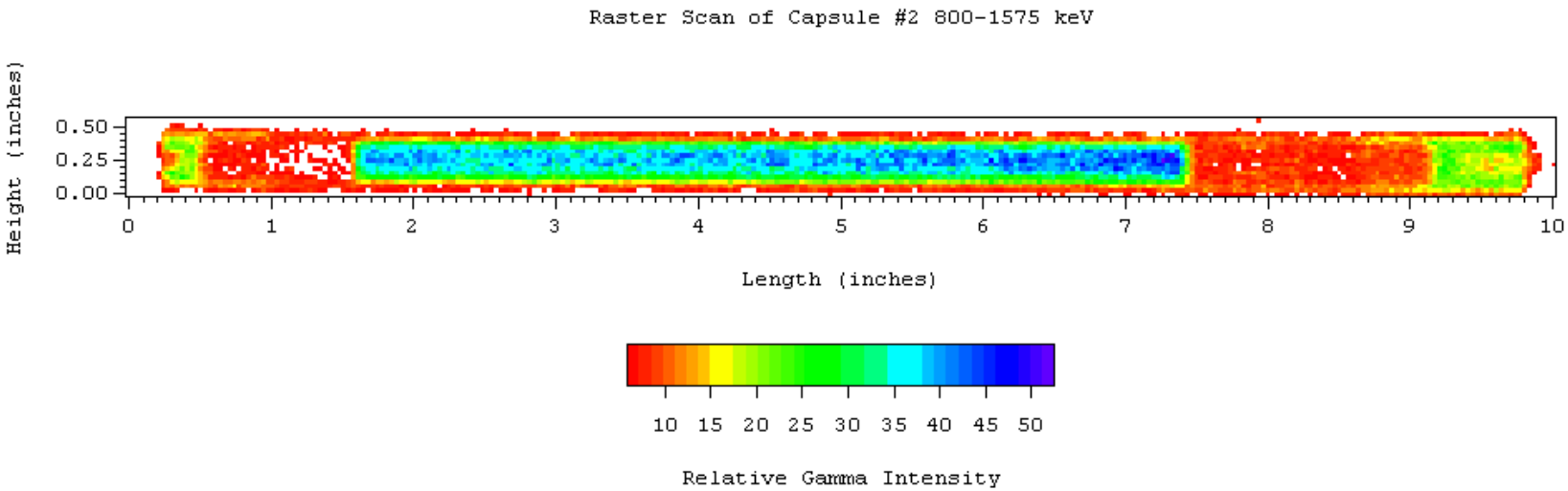

Figure 10 Capsule 2 high energy gamma raster scan. [ras2h.wpg]

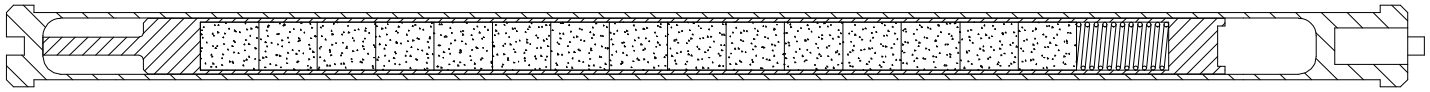

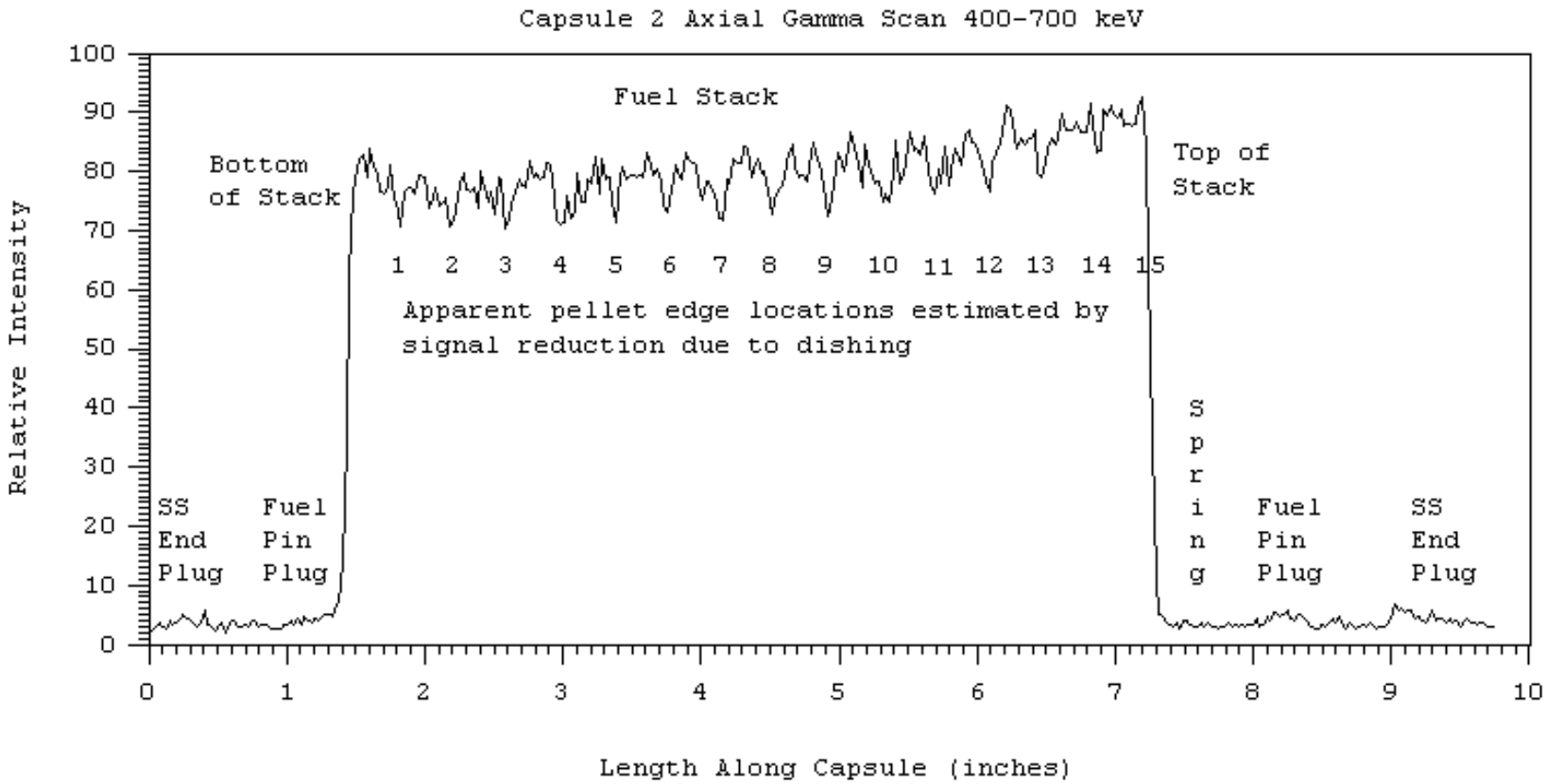

Figure 11 Capsule 2 mid energy gamma line scan. [ls2.wpg]

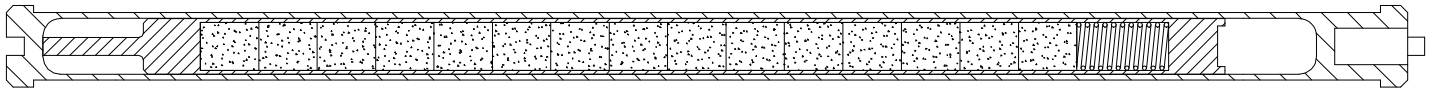

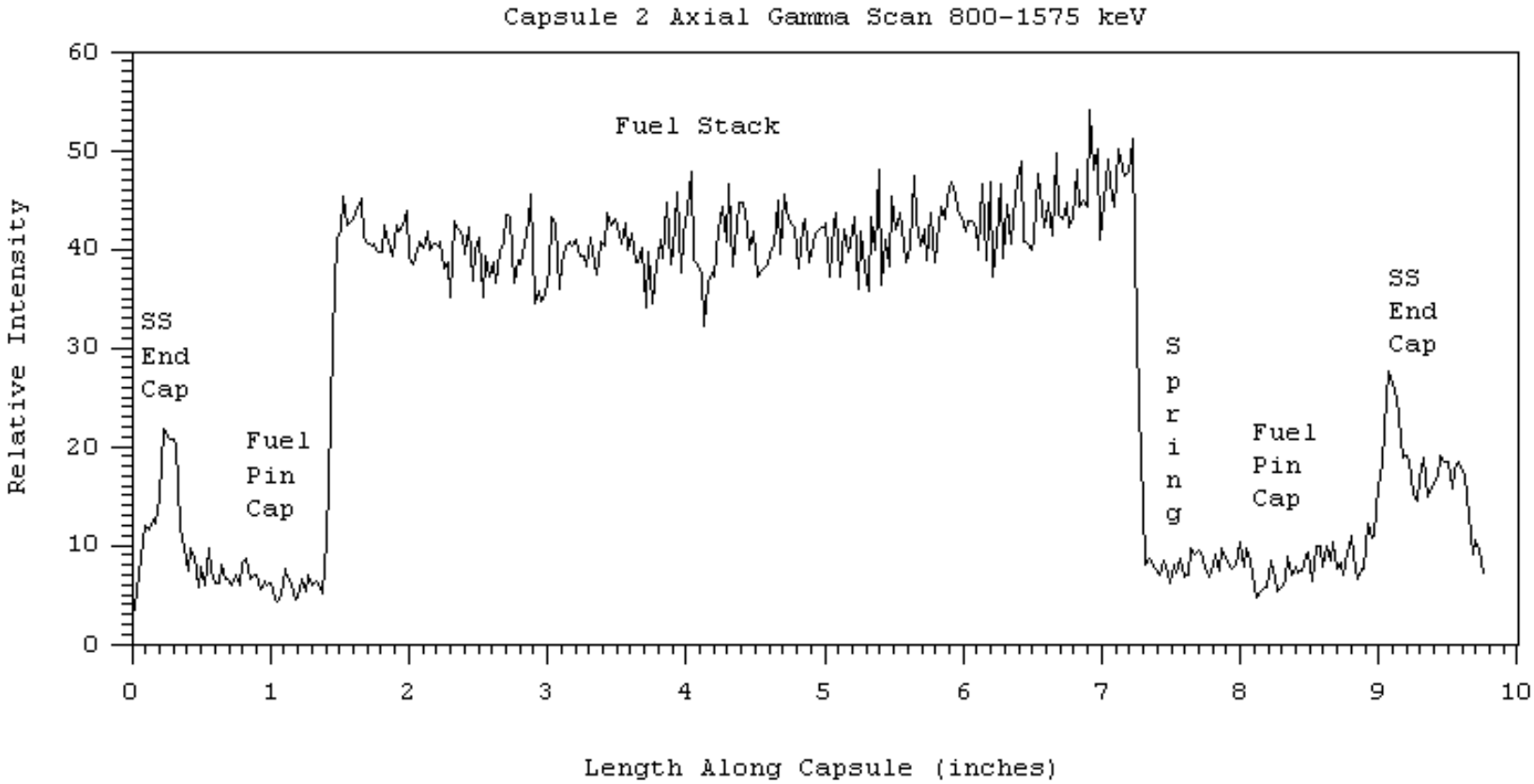

Figure 12 Capsule 2 high energy gamma line scan. [ls2h.wpg]

Overall, the capsule showed no structural problems. All components appeared to be in their proper locations and the fuel pellet stack does not appear to have swelled significantly.

3.4.2 Capsule 9 Gamma Scan

Figure 13 shows the results of the 400 to 700 keV raster scan for Capsule 9. As before, one can make out the stainless steel end caps, the fuel pin end caps, and the fuel pellet stack. Figure 14 shows the same scan in the 800 to 1575 energy range. No inconsistences or abnormalities in internal component locations were noted.

The relative intensities between the two capsules are different because they were scanned approximately two weeks apart. The scanning took place only a few weeks after the end of irradiation, so the contributions of the rapidly decaying short lived isotopes were still important. Thus, the recorded gamma intensity of Capsule 9 is lower because of the extra two weeks of decay time.

Figure 15 shows an axial line scan along Capsule 9 in the 400 to 700 keV energy range. Again, the elements of the capsule are visible. The fuel stack appears to be approximately 5.8 inches long, but in this case the pellet dishing cannot be seen. Apparently, the stronger presence of the shorter lived isotopes helped define the pellet edges in the scan of Capsule 2. Note the burnup peaking at the ends of the fuel stack as was seen before.

Figure 16 shows an axial line scan in the energy range of 800-1575 KeV which accents the stainless steel activation products.

Similar to Capsule 2, Capsule 9 appears to have no major structural problems and all components appear to be in their proper locations with no significant axial fuel swelling.

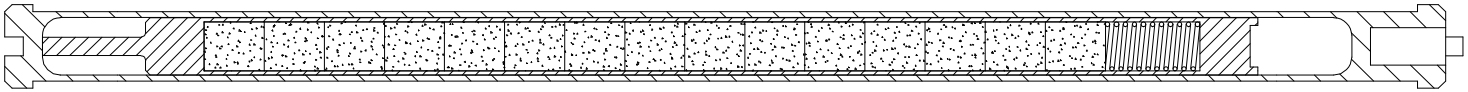

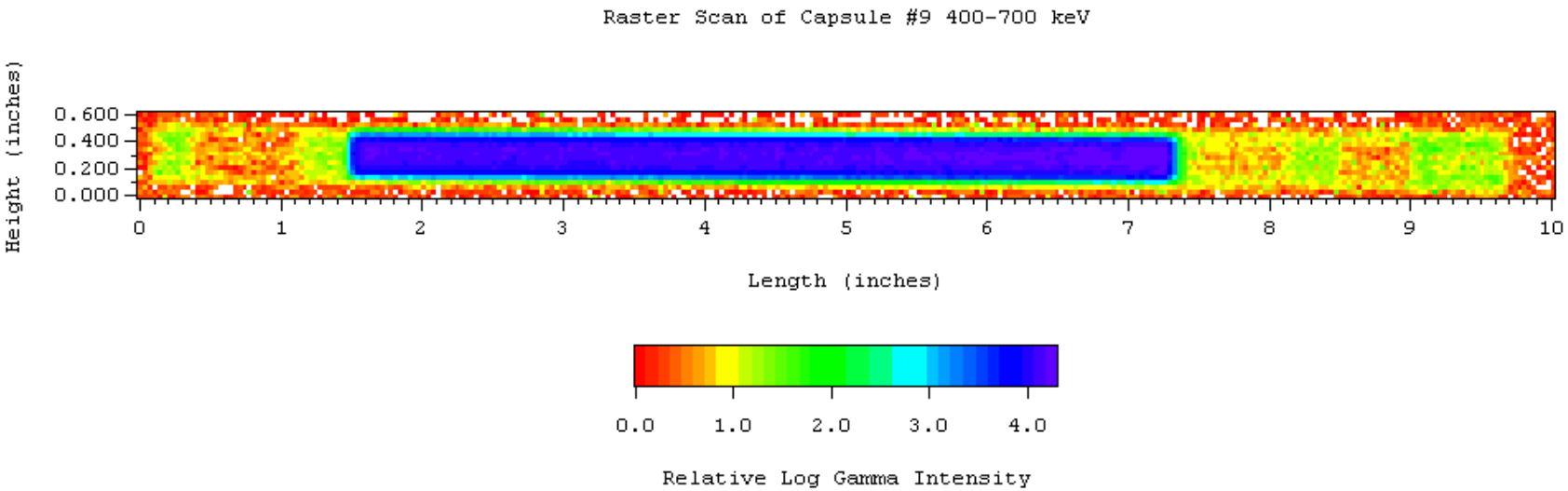

Figure 13 Capsule 9 mid energy gamma raster scan. [ras9.wpg]

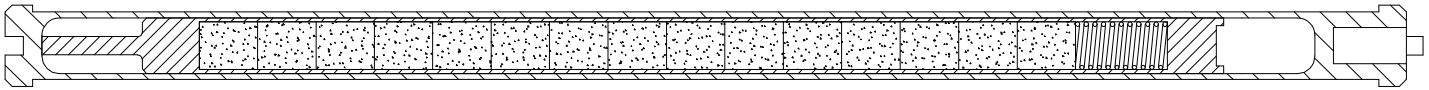

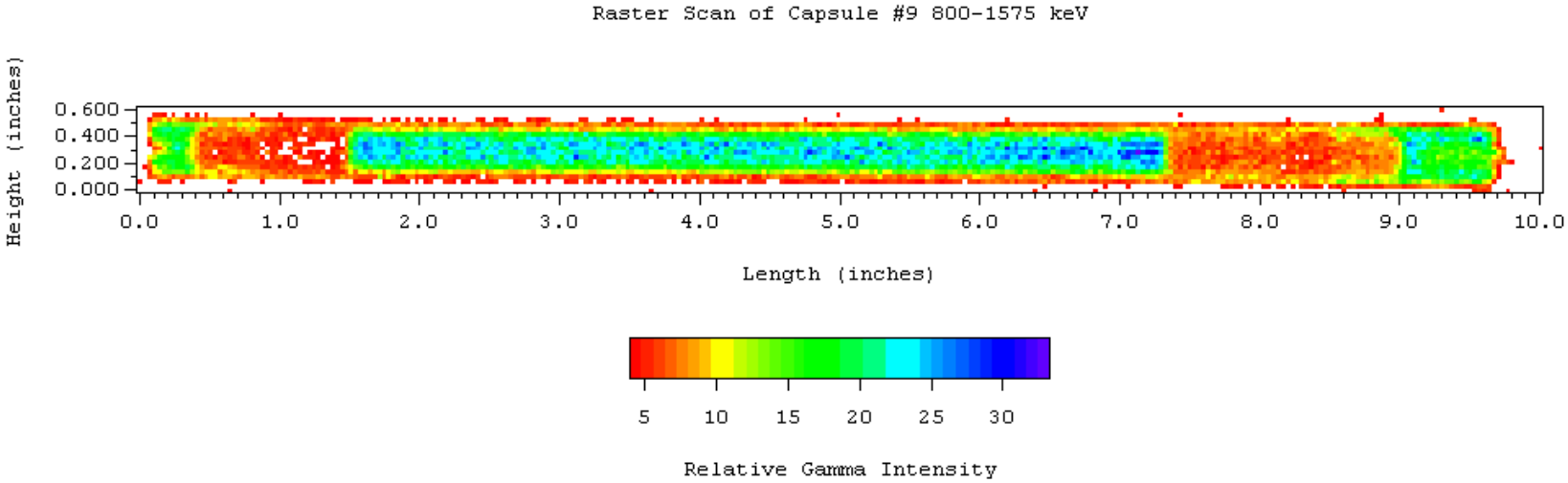

Figure 14 Capsule 9 high energy gamma raster scan. [ras9h.wpg]

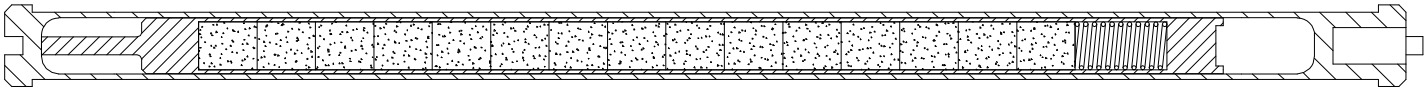

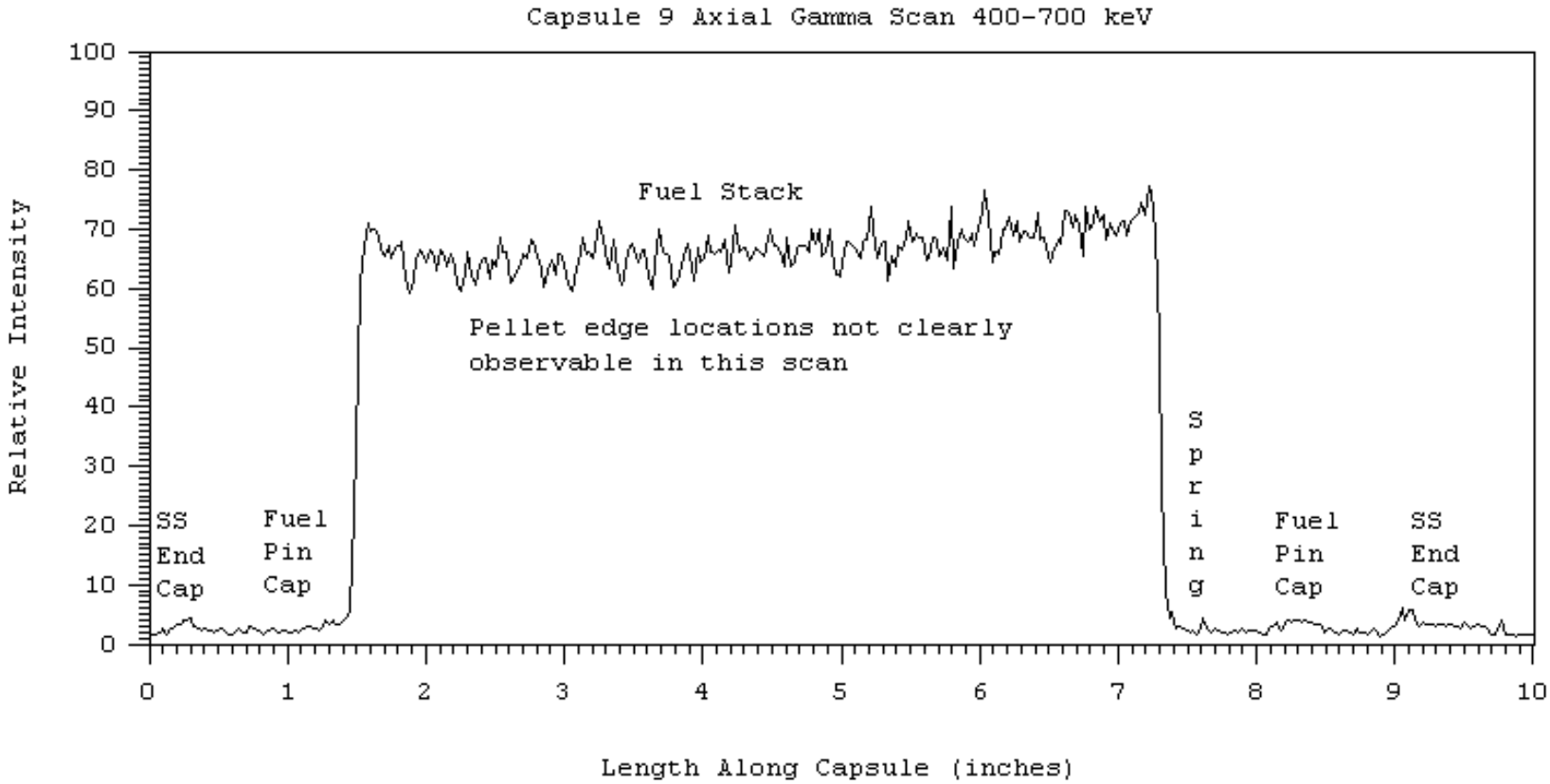

Figure 15 Capsule 9 mid energy gamma line scan. [ls9.wpg]

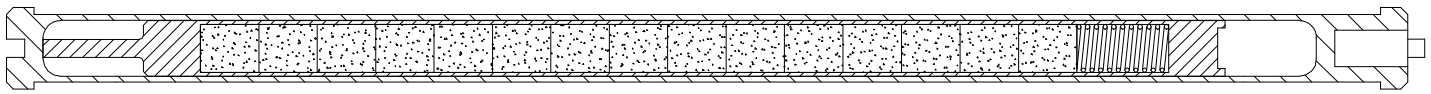

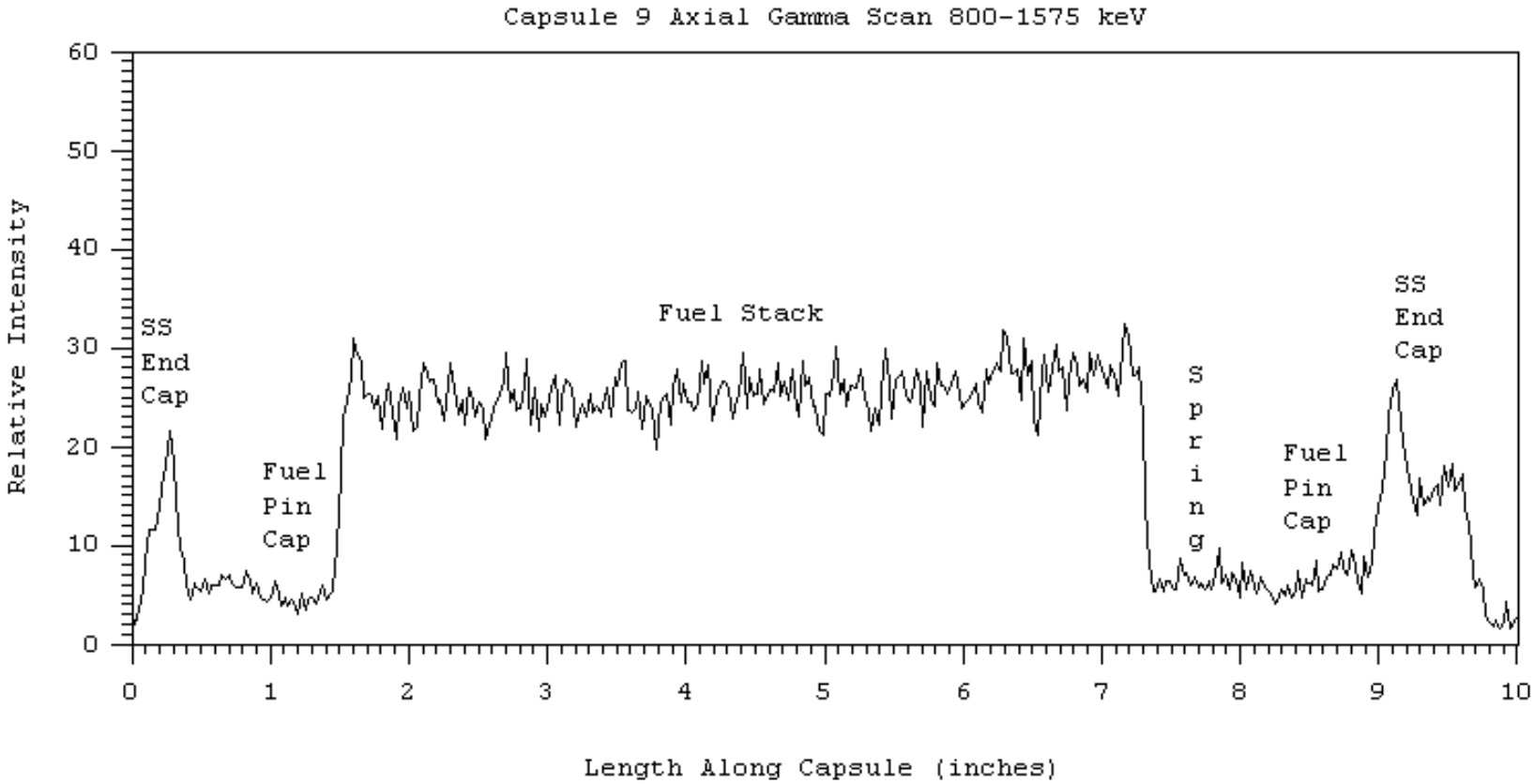

Figure 16 Capsule 9 high energy gamma line scan. [ls9h.wpg]

3.4.3 Gamma Scanner Data Collection Orientation

The gamma intensity data was collected with the alignment lug of the capsule facing the gamma scanner detector as shown in Figure 17.

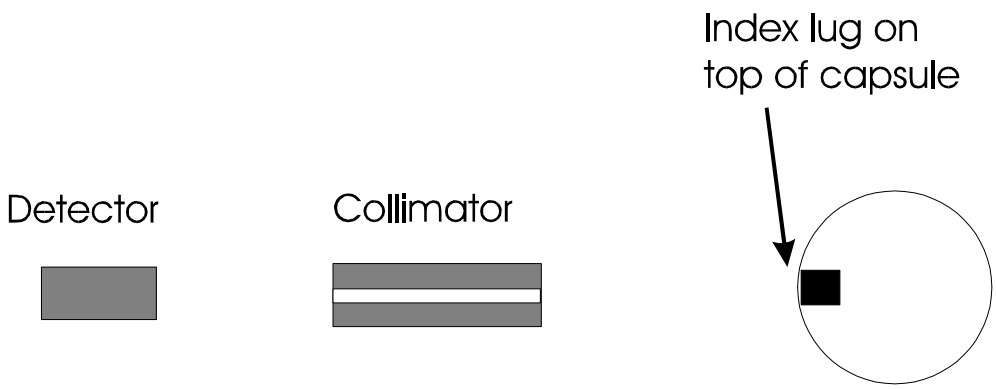

Figure 17 Orientation of the capsule and the gamma scanner collimator/detector. [gamdir.wpg]

3.5 Fission Gas Measurements

The fission gas pressure and ^{85}Kr content in both Capsules 2 and 9 and their associated fuel pins were measured by use of the MOX Fission Gas Pressure Measuring Apparatus. Details of this apparatus and its calibration are described in Ref. 7. Briefly, the apparatus functions by using a vacuum sealed drill-press like action to drill first through the trimmed off top of the MOX capsule and then, after sampling the gas in the capsule upper plenum region, to continue drilling into the contained fuel pin. The drilling stops as each barrier is penetrated to permit measurement of the gas pressure and sweeping of the released gases through a cold trap system to trap and determine the ^{85}Kr quantity. The heart of the apparatus is a ferrofluidic seal which utilizes a novel magnetic fluid for rotary vacuum sealing and a stainless steel bellows for linear vacuum sealing. A diagram of the device is shown in Figure 18.

No anomalous fission gas release was observed in either capsule. The capsule pressures were subatmospheric, as expected since they were sealed at the elevation of INEEL, where the atmospheric pressure is about 12.5 psia. (The actual pressure in the capsule during welding could not be recorded.) The fuel pins were found to be sealed and the fission gas release was found to be in the range of 1.5 to 2.0% (based on ^{85}Kr), with pressures slightly higher than were predicted by the fuel performance code, but well within acceptable limits. No problems occurred with the apparatus. The details are summarized in Table 5.

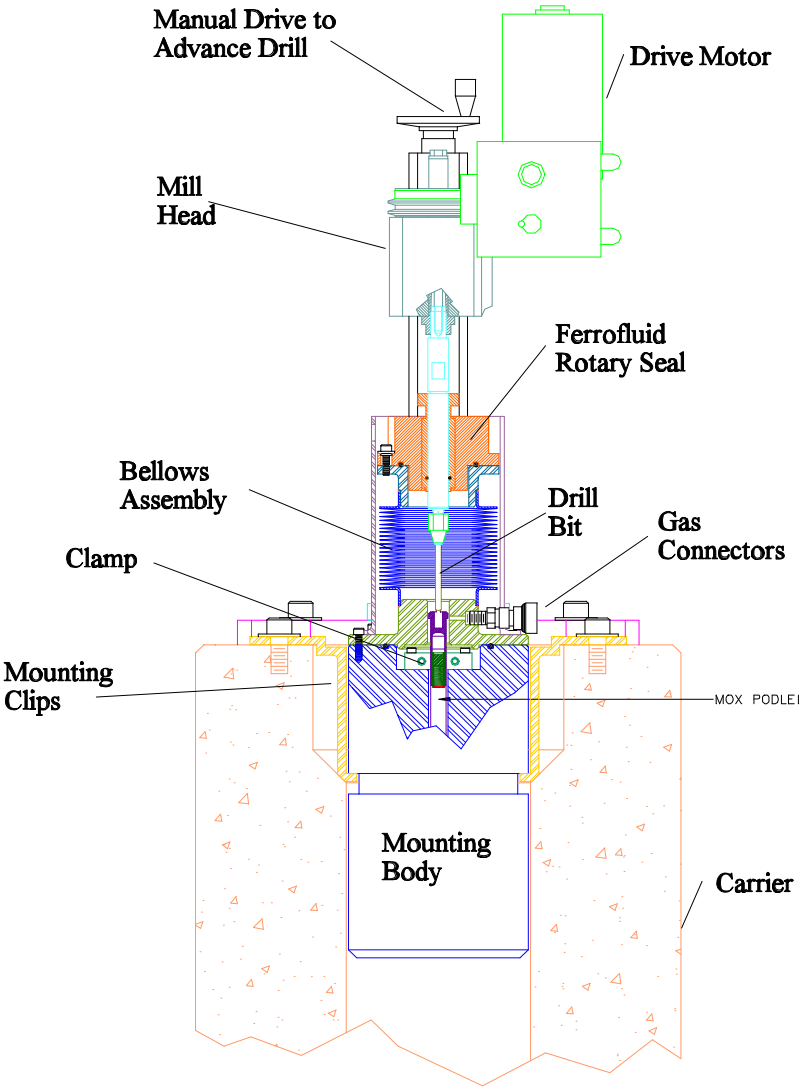

Figure 18 Cross sectional view of the Fission Gas Pressure Measuring Apparatus. [Drill Schematic 2.wpg]

TABLE 5
Fission Gas Measurements

Item	Best Estimate Free Volume[1] (cc)	Measured Pressure (psia)	Measured ^{85}Kr in Free Volume (mCi)	Best Estimate for Total ^{85}Kr Inventory[2] (mCi)	Model Predicted Pressure[3] (psia)	Release Fraction Based on ^{85}Kr Measurement
Capsule 2	2.477	10.1	0.00	0	N/A	N/A
Fuel Pin 5	1.197	23.8	4.38	303	27.5	0.0144
Capsule 9	2.477	10.0	0.00	0	N/A	N/A
Fuel Pin 12	1.225	27.5	5.86	300	27.5	0.0195

[1]Based on actual dimensional measurements and code predicted fuel swelling
[2]Based on ORIGEN calculations (Ref. 6)
[3]Based on CARTS calculations with an estimated release fraction of 0.012 and nominal fuel pellet stack length dimensions (Chapter 2)
Ambient temperature of 23°C
Measured values are approximately ±8% for pressure and ±6% for ^{85}Kr

3.6 Fuel Pin Photo Visual Inspections

Fuel Pin 5 was removed from Capsule 2 by cutting off the bottom of the capsule just above the weld. This operation also removed about ½ of the bottom pedestal of the fuel pin. After deburring the capsule body, the fuel pin was removed by grasping and pulling on the bottom pedestal. The pin slid out easily. After removal, the pin was photographed and measured. The exterior of Fuel Pin 5 was found to be in excellent condition.

No attempt was made to maintain the angular orientation of the fuel pin relative to the capsule index lug because the capsule is free to rotate within the capsule at all times. Photographs of the fuel pin are shown in Figures 19 through 21.

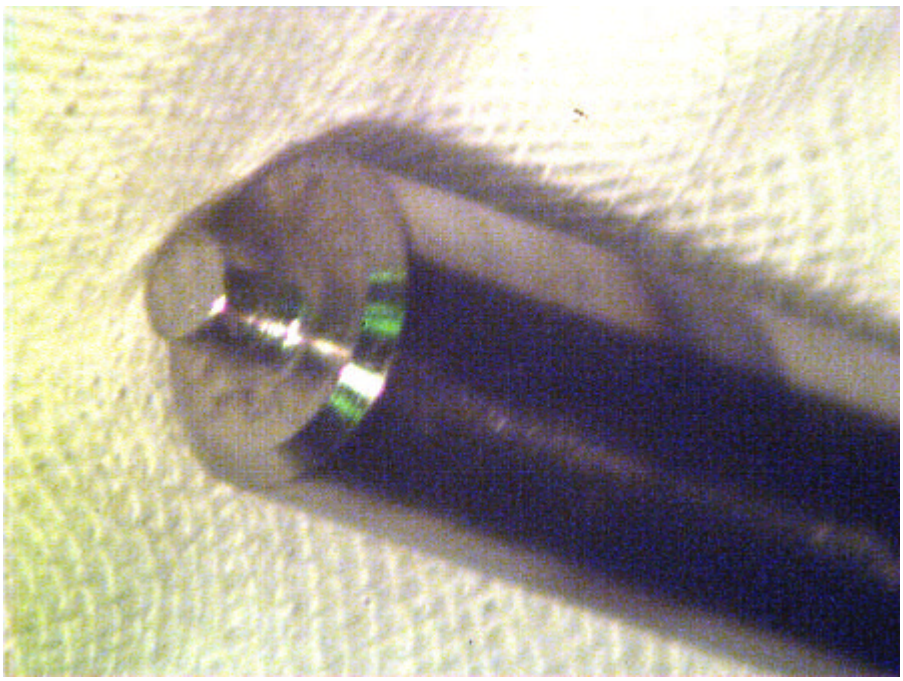

Figure 19 Bottom end of Fuel Pin 5. Note the shortened pedestal from the cutting operation. [P5-bottom.JPG]

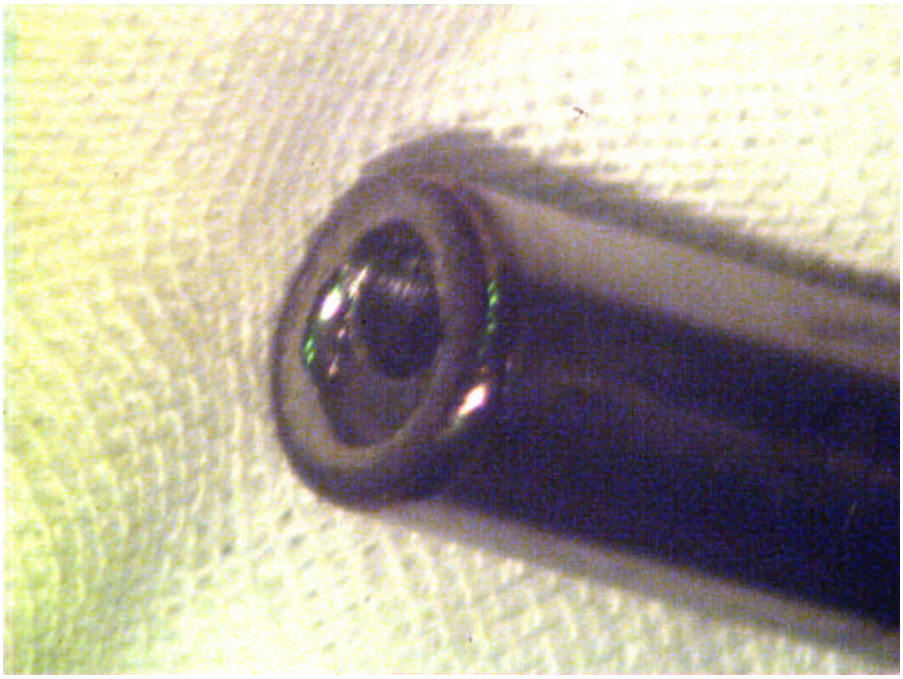

Figure 20 Top end of Fuel Pin 5. Note the hole from the fission gas pressure measurement. [P5-top.JPG]

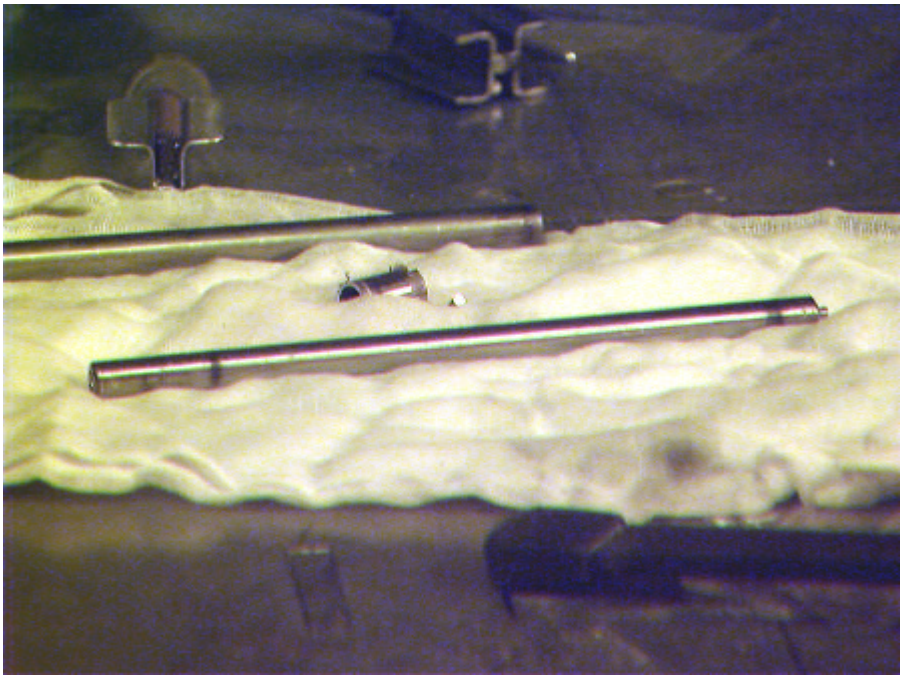

Figure 21 Side view of Fuel Pin 5. Note capsule components in background. [P5-side-front.JPG]

Fuel pin 12 was removed from Capsule 9 in the same manner that Fuel Pin 5 was removed from Capsule 2. The exterior of Fuel Pin 12 was also found to be in excellent condition. Photographs of Fuel Pin 12 are shown in Figs. 22 through 24.

Figure 22 Bottom end of Fuel Pin 12. Note the shortened pedestal from the cutting operations. [P12-bottom.JPG]

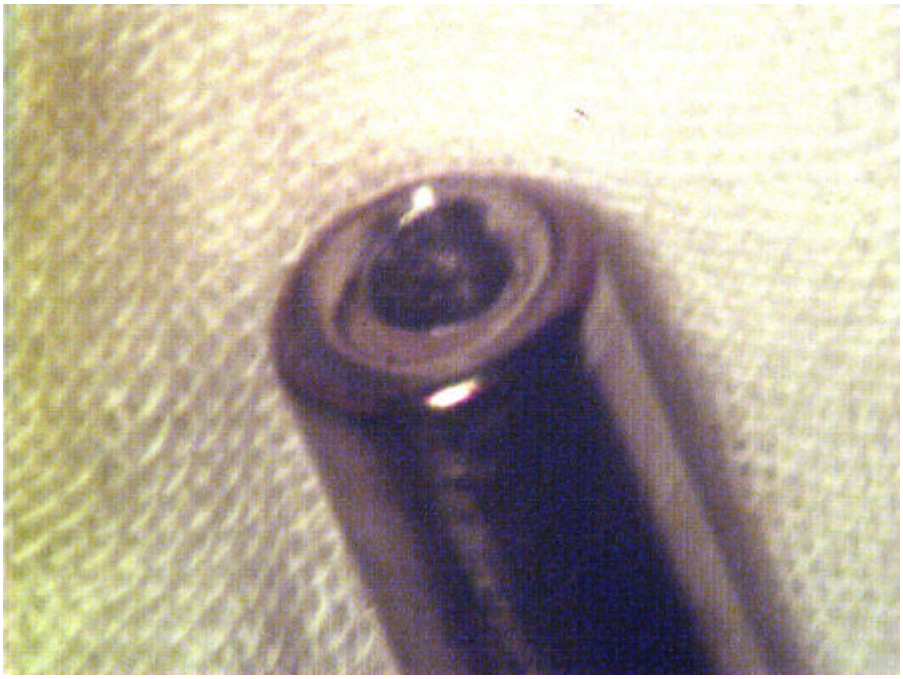

Figure 23 Top end of Fuel Pin 12. Note the hole from the fission gas pressure measurement. It also appears (top of hole) that the drill may have wandered or the pin may have rotated before the drill bit started cutting the hole. [P12-top.JPG]

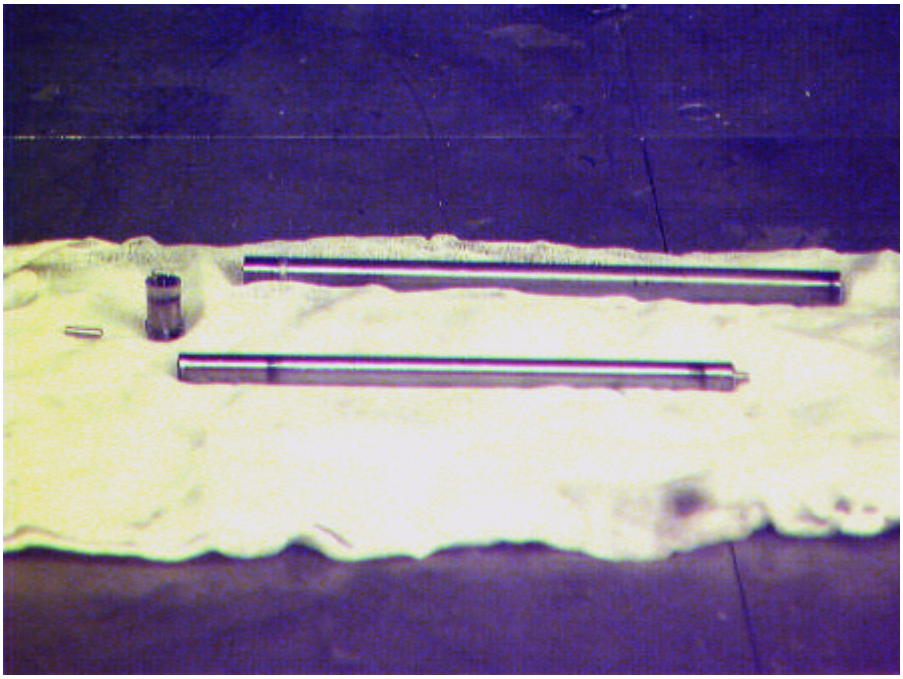

Figure 24 Side view of Fuel Pin 12. Note the capsule components in background. [P12-side-front.JPG]

3.7 Fuel Pin Dimensional Inspections

The results of the fuel pin dimensional inspections are shown in Table 7. For practical purposes, insignificant variations from the preirradiated values were noted. Within 0.001 inches, there were no indications of bowing, out of roundness, or bambooing. No radiation induced dimensional changes were observed in Fuel Pin 5 clad diameter within 0.001 inches. Fuel Pin 12 clad has two spots where the pre/post irradiation diameter difference was greater than 0.001 inches, but less than 0.002 inches. The method of measurement was the same as that shown in Figure 7**.**

In general, Fuel Pin 12 appears to be just slightly larger in diameter than Fuel Pin 5, although a measuring artifact cannot be ruled out because the difference is small and both fuel pins easily slid within their respective (very closely fitting) capsules. In the next stage of the PIE, the internal state of the fuel pins will be examined.

TABLE 7 Fuel Pin Measurements			
Axial Location from Top (inches)	**Diameter Measurement (in) (±0.0005)**		**Preirradiation Values (in)**
	0°	**90°**	
Fuel Pin 5			
0.50	0.3811	0.3810	0.3806 to 0.3808
2.00	0.3811	0.3814	
3.50	0.3814	0.3814	
5.50	0.3805	0.3815	
7.00	0.3805	0.3805	
Fuel Pin 12			
0.50	0.3812	0.3814	0.3806 to 0.3808
2.00	0.3825	0.3824	
3.50	0.3824	0.3814	
5.50	0.3818	0.3817	
7.00	0.3814	0.3815	
Length (in) (±0.005)			
Fuel Pin 5	7.413		7.41 less pedestal
Fuel Pin 12	7.413		7.41 less pedestal
Mass (g) (±0.1g)			
Fuel Pin 5	111.2		Not given
Fuel Pin 12	111.7		Not given

4.0 CONCLUSIONS FROM PRELIMINARY PIE

Capsules 2 and 9 were visually and dimensionally examined. No signs of capsule damage or distortion were observed. Both capsules were gamma scanned and showed no signs of structural irregularities.

After a sufficient period of time was allowed for the required ^{131}I decay, the capsules were drilled to sample their gas plenums and the free volumes in their associated fuel pins. The gas measurements were in the expected pressure range and the implied fission gas release fractions were in the range of 1.5 to 2.0%, slightly higher than assumed for the best-estimate calculations, but well within expected limits.

The capsules were opened and the fuel pins removed. No signs of damage or distortion of the fuel pin's clad were observed. In fact, the fuel pins easily slid out as predicted by the CARTS code calculations.

Overall, Capsule 2 and Capsule 9 handled the irradiation without incident and there are no indications of any mechanisms that might threaten the containment integrity of the sister capsules currently continuing their irradiation in the ATR.

5.0 ACKNOWLEDGMENTS

The authors wish to thank Steve Childs, Charlie DeVore, Pat Howard, Tom Kenney, and Jeff Moody of the Irradiated Fuels Examination Laboratory Staff for their help with the MOX capsule PIE task. We also wish to thank Larry Ott for modeling support.

6.0 REFERENCES

1. B.S. Cowell and S.A. Hodge, *Fissile Materials Disposition Program Light-Water Reactor Mixed Oxide Fuel Irradiation Test Project Plan*, ORNL/TM-13419, Rev 1, Feb 1998

2. R.N. Morris, C.A. Baldwin, C.M. Malone, N.H. Packan, *MOX Average Power Early PIE: 8 GWd/MT Quick Look*, ORNL/MD/LTR-163 Rev. 1, February 1999

3. R.N. Morris, et. al., MOX Average Power Early PIE: 8 GWd/MT Final Report, ORNL/MD/LTR-172, November 1999

4. R.N. Morris, *MOX Capsule Post-Irradiation Examination Vol. I: Test Plan for Low Burnup Fuel*, ORNL/MD/LTR-93, August 1997

5. S.A. Hodge, *Fission Gas Release and Pellet Swelling Within the High-Power Mixed-Oxide Irradiation Test Assembly*, ORNL/MD/LTR-128 Rev. 1, November 1998

6. W.K. Terry, *As-Run Radiological Characterization of MOX Fuel Capsules Removed From the ATR After Cycle 120A - WKT-04-99*, November 8, 1999

7. R.N. Morris, C.A. Baldwin, C.M. Malone, *MOX Fission Gas Pressure Measuring Apparatus*, ORNL/MD/LTR-176, January 2000

7.0 DISTRIBUTION

1. P.T. Rhoads, U.S. Department of Energy, MD-3, 1000 Independence Avenue SW, Forrestal Building 6G-050, Washington DC 20585
2. J. Thompson, U.S. Department of Energy, MD-3, 1000 Independence Avenue SW, Forrestal Building 6G-050, Washington DC 20585

3-7. D. Alberstein, Los Alamos National Laboratory, P.O. Box 1663, Los Alamos, NM 87545

8-12. R.C. Pedersen, Idaho National Engineering and Environmental Laboratory, EROB, 2525 Fremont Avenue, Idaho Falls, ID 83415-3419

13. P. Kasik, MPR Associates Inc., 320 King Street, Alexandria, VA 22314-3238

14. C.A. Baldwin

15. B.S. Cowell

16. S.R. Greene

17-21. S.A. Hodge

22. L.L. Horton

23. M.W. Kennard, Stoller Nuclear Fuel, 485 Washington Avenue, Pleasantville, NY 10570

24.-28. L.L. Losh, Framatome Cogema Fuels, 3315 Old Forest Road, Lynchburg, Va 24506

29.-33. C.M. Malone

34.-38. R.N. Morris

39. L.J. Ott

40. D.J. Spellman

41. K.R. Thoms

42. ORNL Laboratory Records (RC)